Available online at www.sciencedirect.com
SCIENCE DIRECT
Polymer 47 (2006) 3486–3493
polymer
www.elsevier.com/locate/polymer

Positron/positronium annihilation as a probe for chemical environments of free volume holes in fluoropolymers

D. Bamford [a], G. Dlubek [a,b,*], G. Dommet [a], S. Höring [c], T. Lüpke [d], D. Kilburn [a], M.A. Alam [a]

[a] H.H. Wills Physics Laboratory, University of Bristol, Tyndal Avenue, Bristol BS8 1TL, UK
[b] ITA Institut für Innovative Technologien, Köthen, Aussenstelle Halle, Wiesenring 4, D-06120 Lieskau (bei Halle/S), Germany
[c] Martin-Luther-Universität Halle-Wittenberg, Fachbereich Chemie, Institut für Technische und Makromolekulare Chemie, D-06099 Halle/S, Germany
[d] Martin-Luther-Universität Halle-Wittenberg, Fachbereich Ingenieurwissenschaften, D-06099 Halle/S, Germany

Received 19 October 2005; received in revised form 31 January 2006; accepted 13 March 2006
Available online 3 April 2006

Abstract

The sensitivity of the Doppler-broadening of positron annihilation radiation (DBAR) for the chemical environment of free volume holes was studied for fluorinated polymers. The free volume was characterized by positron annihilation lifetime spectroscopy (PALS). For this study, we prepared three series of copolymers of methacrylates with various semi-fluorinated methacrylates with increasing fractional number of fluorine atoms f_F. Moreover some commercial fluoroelastomers and semicrystalline fluoropolymers were investigated. After the subtraction of a narrow para-positronium DBAR component, calculated on a simplified way using the PALS data, from the conventional Doppler broadened annihilation energy line, the remaining broad distribution shows no response to the size of free volume holes or the positronium formation probability but can be related to the nature and density of the chemical species in the vicinity of the holes. Element specific information of the annihilation site can be expressed in terms of an integral parameter, e.g. the normalised curve shape parameter S_b^n of the broad DBAR component. We observed that S_b^n does not show the expected exponential decrease but goes down linearly with f_F in the range $f_F < 0.45$ and levels-off for $f_F \geq 0.5$. This was explained assuming positronium localization and annihilation in two types of holes: holes, which have walls free of fluorine atoms and holes, which contain fluorine in their walls. A steeper, exponential-like decrease of S_b^n with f_F seem to occur for the fluoroelastomeric and semicrystalline fluoropolymers which contain not less than one F atom per two backbone carbons. In this, the case *ortho*-positronium localized at a hole will always find at least one fluorine atom in which neighbourhood it can annihilate.

Keywords: Free volume; Positron annihilation; Fluoropolymers

1. Introduction

The positron annihilation lifetime spectroscopy (PALS) has found increasing interest and growing application for studying polymeric materials during recent years [1–6]. The reason for this is that it provides a unique probe for sub-nanometre local free volumes in amorphous polymers that arise from their structural disorder. Such free volume holes play a crucial role in determining a variety of properties of polymers, e.g. in the permeation of gas and liquid through such materials, changes in their behaviour under pressure, temperature and under the influence of plasticizers and in their general mechanical and rheological properties [7,8].

In molecular materials, the positron preferentially forms and annihilates from a bound state called positronium (Ps). The Ps forms either in the so called para (anti-parallel electron and positron spins: *p*-Ps) or ortho (parallel electron and positron spins: *o*-Ps) positronium states with a relative abundance of 1:3 [1,6]. In vacuum, a *p*-Ps has a lifetime 125 ps and annihilates via 2 γ-photons while an *o*-Ps lives ∼142 ns and annihilates via 3-γ. When within the free volume in polymers, the *o*-Ps has a finite probability of annihilating with an electron other than its bound partner (and of opposite spin) during the numerous collisions that it undergoes with the molecules of the surroundings, a process generally termed as the 'pick-off'. The result is a drastically reduced *o*-Ps lifetime compared to its vacuum value and its annihilation in 2-γ. This *o*-Ps lifetime mirrors extremely sensitive the electron density in the nearest surroundings of the Ps and on this way the size of free volume holes where *o*-Ps is localized and its variation [1–6].

* Corresponding author. Address: ITA Institut für Innovative Technologien, Köthen, Aussenstelle Halle, Wiesenring 4, D-06120 Lieskau (bei Halle/S), Germany. Tel.: +49 345 5512902; fax: +49 40 3603241.
E-mail address: gdlubek@aol.com (G. Dlubek).

0032-3861/$ - see front matter © 2006 Elsevier Ltd. All rights reserved.
doi:10.1016/j.polymer.2006.03.044

In previous works [9,10] we have demonstrated that the measurement of the energy distribution of the 2-γ annihilation radiation, by using a high-resolution Ge semiconductor detector may potentially act as a chemical probe of polymers and other molecular materials. The 0.511 keV annihilation line is broadened due the Doppler shift of the γ-rays and mirrors the momentum density of the annihilating electron-positron pairs. This method, known as Doppler-broadening of annihilation radiation (DBAR, [1,6]), is usually employed to study vacancy defects in compounds and decomposition processes in metallic alloys [11–13]. The method appears, however, also as an interesting and important counterpart of the PALS experiments in polymer studies [9,10,14].

While the annihilation of positrons (e^+) and the pick-off of *o*-Ps occurs with the electrons of the atoms and molecules of the material, *p*-Ps annihilates via self-annihilation (i.e. the positron annihilates with the own *p*-Ps electron) almost without any sensitivity to the chemistry of the sample. Therefore, it is necessary to subtract the *p*-Ps component from the total DBAR distribution.

p-Ps self-annihilation produces a part of the annihilation radiation spectrum that has a smaller width than the parts coming from e^+ and *o*-Ps pick-off annihilation. This part of the DBAR curve is known in the literature as 'narrow component' [6]. In our previous works, we have demonstrated that through the fitting of three Gaussians to the DBAR curve this narrow component can be identified as the narrowest of the three Gaussians and subtracted from the total spectrum [9,10]. The remaining 'broad component' comes from the annihilation of positrons (e^+) and pick-off of *o*-Ps with bound electrons and reflects therefore the electronic configuration of atoms and molecules forming the polymer. It shows no correlation to the spatial dimensions of the holes but exhibits an enhanced sensitivity to the presence and number densities of various types of atoms in the walls of the holes. The broad component shows also little correlation to the positronium yield since the curves from the e^+ and *o*-Ps annihilation are of similar shape [9,10,15].

We observed that the DBAR broad components of a large variety of hydrocarbon polymers are very similar in their shape [9,10]. When, however, other elements, such like oxygen, chlorine, or fluorine are contained in the polymer the curves can distinctly broaden. The maximum of the broad distribution (peak height) normalized to the unity area below the curve seems to decrease exponentially with the content of these elements. The specific decrease of the peak height depends on the type of atoms and is strongest for fluorinated polymers [9].

In this work, we study the chemical sensitivity of the DBAR method and focus our activities to fluorinated polymers. For our study, we prepared various fluorinated copolymers, their monomers were chosen as they allowed a series of polymers with a wide range of fluorine contents to be easily produced. The monomers were also selected to be structurally and chemically similar, except for the replacement of a number of hydrogen atoms by fluorine atoms, and so there should be as little difference as possible between the copolymers apart from their chemical composition.

We utilised measurements of the Doppler-broadened annihilation radiation, and, for estimating the size of free volume holes and their variation with the type and composition of the copolymers, of the positron annihilation lifetime spectrum. For the correction of the DBAR curve with respect to the *p*-Ps narrow component we used a simplified and easily to handle, but sufficiently accurate procedure. Supplementary to the positron experiments we measured the temperature of the glass transition using the differential scanning calorimetry.

2. Experimental

2.1. Samples

A large number of copolymers with varying fluorine content were prepared, the chemical structure of their comonomers is shown in Scheme 1 and their composition, the glass transition temperature T_g, and the PALS data are compiled in Table 1. Differential scanning calorimetry measurements were performed with a heat flux calorimeter, DSC 820 (Mettler–Toledo), calibrated with indium and zinc. The T_g was estimated as the midpoint (half change) of the corresponding stage in the second heat flow curves (heating rate of 10 K/min) according to ISO 11357-2.

First, a series of butylmethacrylate–heptafluorobutylmethacrylate (BMA/HFBMA) copolymers were prepared which ranged from pure poly(butylmethacrylate) to pure poly(heptaflurobutylmethacrylate). In these polymers, the electronegative fluorine atoms are sufficiently far away from the reactive methacrylate group that the reaction rate of the two monomers should be the same, allowing an azeotropic reaction with random incorporation of the monomers in the final copolymer.

The butylmethacrylate and heptafluorobutylmethacrylate monomers (Scheme 1(a) and (b)) obtained from Aldrich, were first purified to remove the hydroquinone stabiliser by stirring with inhibitor remover beads (Aldrich 30,631–2) for 8 h in an atmosphere of pure nitrogen, replacing the beads every 2–3 h. The monomers were mixed by weight according to the composition required and placed in a narrow glass tube with 0.1% by weight 2,2′-azo-bis-(2-methylpropionitrile) from Aldrich as initiator. The polymerisation occurs via free radical polymerisation and is terminated by the presence of oxygen. For this reason, the mixture was de-gassed using a series of freeze, evacuate, thaw cycles. Firstly the mixture was frozen by immersion in liquid nitrogen, then evacuated to <0.01 Pa. The tube was isolated from the vacuum and allowed to thaw. The cycle was repeated ($\sim$5–10 times) until no further gas was evolved upon thawing. Finally, the mixture was frozen, then evacuated and the top of the glass tube sealed using a blowtorch.

The tubes were placed in a heat bath at 50 °C for >12 h to allow complete polymerisation to occur. The degree of polymerisation was check using Raman spectroscopy by comparing the intensity of the carbon double-bond carbon

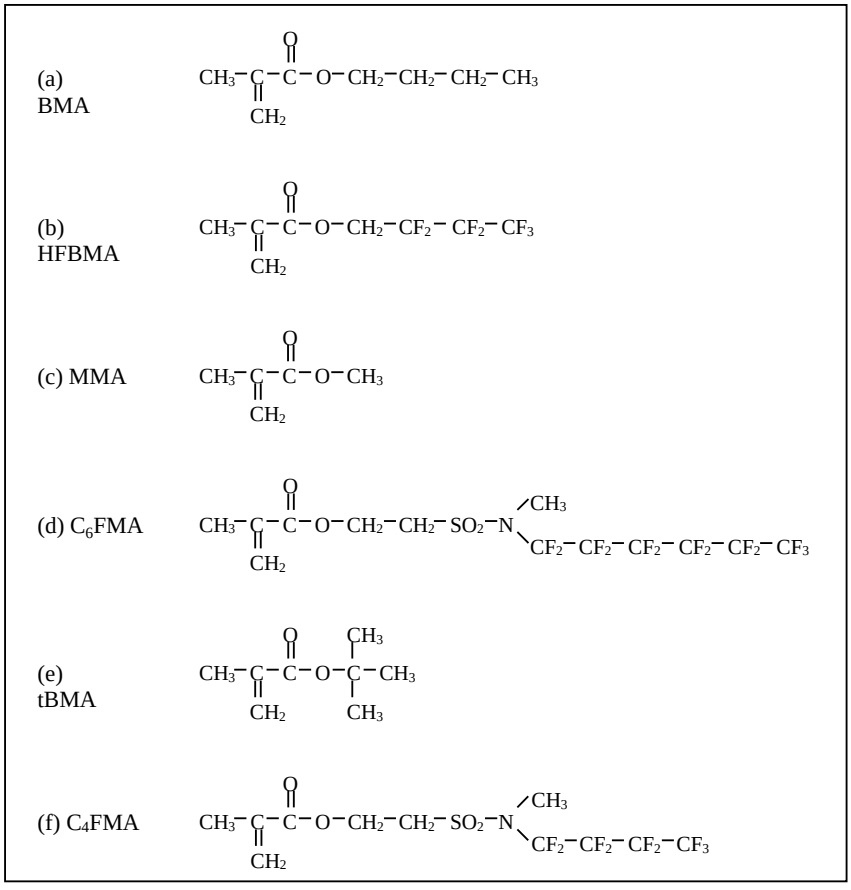

Scheme 1. Chemical structure of (a) butyl-methacrylate (BMA), (b) hepta-fluoro-butyl-methacrylate (HFBMA), (c) methyl-methacrylate (MMA), (d) 2-(*N*-methyl-perfluorohexansulfonamide)ethyl-methacrylate (C_6FMA), (e) *tert*-butyl-methacrylate (tBMA) and (f) 2-(*N*-methyl-perfluorobutansulfonamide)ethyl-methacrylate (C_4FMA).

Table 1
Summary of the chemical structure and the fractional number of F-atoms of the fluorinated copolymers and the key values determined from DBAR (raw curve-shape parameter *S*, corrected parameter S_b^n), PALS (*o*-Ps lifetime τ_3, hole radius r_h and intensity I_3), and DSC (T_g from second heat) measurements

Sample name	T_g (°C) (±2)	Fraction of F (±0.004)	*S* (raw) (±0.002)	S_b^n (corr.) (±0.002)	τ_3 (ps) (±30)	r_h (Å) (±0.02)	I_3 (%) (±1)
BMA	39.7	0	0.489	0.468	2547	3.315	31
BMA/HFBMA 16.5	48.0	0.048	0.483	0.463	2643	3.388	29
BMA/HFBMA 20.0	49.8	0.058	0.482	0.462	2720	3.444	28.4
BMA/HFBMA 39.5	58.1	0.115	0.475	0.455	2998	3.635	26.8
BMA/HFBMA 60.9	58.5	0.178	0.469	0.450	3230	3.780	25.3
BMA/HFBMA 79.0	54.5	0.231	0.464	0.445	3637	4.006	23.9
HFBMA	56.4	0.292	0.459	0.437	3588	3.981	26.5
MMA	107.1	0	0.481	0.466	2106	2.950	30.0
MMA/C6FMA 15.7	98.0	0.104	0.471	0.456	2324	3.138	23.1
MMA/C6FMA 29.5	118.7	0.163	0.468	0.453	2599	3.355	21.5
MMA/C6FMA 43.9	95.6	0.206	0.464	0.451	2866	3.547	17.7
MMA/C6FMA 63.6	82.9	0.247	0.461	0.447	3254	3.795	19.1
tBMA	114.3	0	0.488	0.469	2518	3.293	28.6
tBMA/C4FMA 10.0	115.5	0.035	0.477	0.464	2666	3.405	21
tBMA/C4FMA 53.0	100.7	0.152	0.464	0.45	2848	3.534	20.4
TFE/PMVE	−2	0.643	0.427	0.421	3506	3.938	15.1
VDF/HFP 22	−18	0.406	0.429	0.424	2770	3.481	12.5
VDF/HFP	−17.1	0.561	0.424	0.419	2605	3.359	9.1
VDf/TFE/HFP	−15.0	0.584	0.423	0.418	2779	3.486	9.4
HDPE	n.d.	0	0.511	0.499	2409	3.204	20.9
PVF	n.d.	0.167	0.431	0.426	2232	3.060	10.2
PVDF	n.d.	0.333	0.437	0.428	2217	3.047	14.4
PTFE	n.d.	0.667	0.436	0.427	2847	3.534	14

C=C peak at 1650 cm^{-1} to the carbon double-bond oxygen C=O peak at 1720 cm^{-1}. For the final samples, there was no C=C peak observable, showing the polymers to be completely polymerised.

Two further series of copolymers of methylmethacrylate with 2-(*N*-methyl-perfluorohexansulfonamide)ethyl-methacrylate (MMA/C6FMA) (Scheme 1(c) and (d)) and tert-butylmethacrylate with 2-(*N*-methyl-perfluorobutansulfonamide)ethyl-methacrylate (*t*BMA/C4FMA, Scheme 1(e) and (f)) were made. These samples were prepared from mixtures of the approximate monomers at 50 °C in a solution of tolulene and acetone with an initiator concentration of 0.5% by weight.

Two commercial fluoroelastomer samples were obtained from Dyneon GmbH and Co. KG, Germany (a 3M Company). One elastomer is a copolymer of tetrafluoroethylene(–[C_2F_4]–) and perfluoro(methyl vinyl ether)(–[F_2C–$CF(OCF_3)$]–, TFE/PMVE, content of PMVE = 15–55 mol%), denoted as Dyneon™ Perfluoroelastomer PFE. The other elastomer is a copolymer of vinylidene fluoride(–[CF_2CH_2]–) and hexafluoropropylene(–[F_2C–$CF(CF_3)$]–, VDF/HFP 22 mol%), denoted as Fluorel™ FC-2175. PALS measurements on these samples were discussed in detail in a previous work [16]. Two further fluoroelastomers of vinylidene fluoride with hexafluoropropylene, VDF/HFP, known as Tecnoflon N535, and with tetrafluoroethylene and hexafluoropropylene, VDF/TFE/HFP, known as Tecnoflon TN80 were studied (the exact composition of these samples are known to the authors). Moreover, semicrystalline polymers of poly(vinylfluoride), PVF, poly (vinylidenefluoride), PVDF, and poly(tetrafluoroethylene), PTFE, were investigated. The last five polymers were obtained from Ausimont Inc., USA. Moreover, we studied a high-density polyethylene (PE) having a crystallinity of ~60%.

2.2. PALS and DBAR measurements

For each of the samples, both PALS and DBAR measurements were performed at room temperature. The PALS experiments were carried out using a fast–fast coincidence system [1,6] with a time resolution of 248 ps (FWHM, Na^{22} source) and a channel width of 50.0 ps. The specimens were platelets of 8×8 mm^2 in area and 1.5 mm in thickness. For each experiment, two identical samples were sandwiched around a 5×10^6 Bq positron source (^{22}Na), prepared by evaporating carrier-free ^{22}NaCl solution on a Kapton foil of 8 μm thickness. Well annealed aluminium platelets ($\tau = 162$ ps) were studied as a reference material for estimating the resolution FWHM and the positron source correction of 340 ps (9.2%) and 2500 ps (0.24%). A total of 5×10^6 counts were measured for each sample. The DBAR measurements [1,6] were performed by using a high resolution intrinsic Ge detector system with an operational resolution of 1.30 ± 0.05 keV at the photo peak of 511 keV. The channel width was 0.123 keV. For each of the measurements a total of 7×10^6 counts in the annihilation peak were collected.

2.3. Data analysis

For the analysis of the lifetime spectra we used the discrete-term routine LIFSPECFIT [17] and the routine MELT [18]. MELT inverts the lifetime spectrum into a continuous lifetime distribution using a quantified maximum entropy method. The lifetime distributions obtained for the amorphous samples exhibit three well separated peaks. The peaks have mass centres at $\tau_1 \approx 150$ ps, $\tau_2 = 350$–420 ps, and $\tau_3 = 2000$–2600 ps. The smallest two lifetimes are attributed to *p*-Ps and free positron (e^+, not Ps) annihilation while the longest lifetime is due to *o*-Ps pick-off annihilation. For the final analysis of lifetime spectra we used the routine LIFSPECFIT assuming three discrete exponential lifetime components [1,6]. This routine delivers lifetime parameters with higher statistical accuracy than those got from MELT. We are most interested in the *o*-Ps annihilation parameters which are shown in Table 1 and Fig. 1.

As mentioned Ps is formed and localized at sub-nanometre size holes of the free volume. In a simple semi-empirical model it is assumed that the Ps is confined in an infinitely high square well potential with the radius $r_h + \delta r$ where r_h is the radius of the hole assumed to be spherical and the empirically determined $\delta r = 1.66$ Å describes the penetration of the Ps wave function into the hole walls. It follows from elementary quantum mechanics that the observed *o*-Ps pick off lifetime $\tau_{po} = \tau_3$ can be related to the radius of the hole r_h as [5,19,20]

$$\tau_{po} = 0.5\ \text{ns}\left[1 - \frac{r_h}{r_h + \delta r} + \frac{1}{2\pi}\sin\left(\frac{2\pi r_h}{r_h + \delta r}\right)\right]^{-1}. \quad (1)$$

The prefactor of 0.5 ns is the inverse of the spin-averaged Ps annihilation rate [1,6].

The DBAR spectra were analysed in two steps. As a first step, the spectra were symmetrised by subtracting a non-linear background function (see [6], p. 44) fitted to the background on

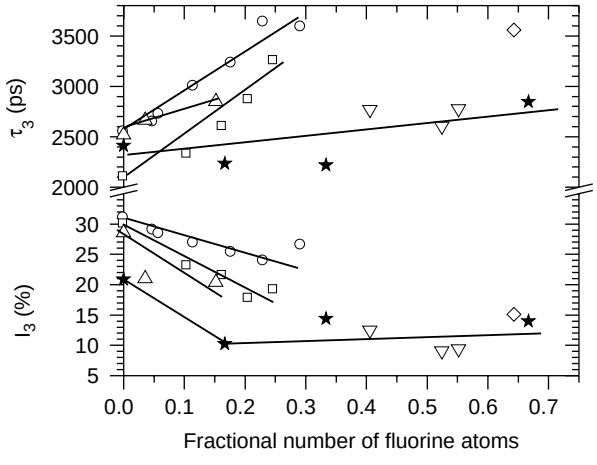

Fig. 1. The *o*-Ps lifetime τ_3 and the intensity I_3 for fluoropolymers as a function of the fractional number of fluorine atoms. (Circles) BMA/HFBMA, (squares) MMA/C6FMA, (up-triangles) tBMA/C4FMA, (down-triangles) fluoroelastomers VDF/HFP 22, VF/HFP, VF/TFE/HFP, (diamond) TFE/PMVE, (filled stars) semicrystalline PE, PVF, PVDF, PTFE. The lines through the data are a visual aid.

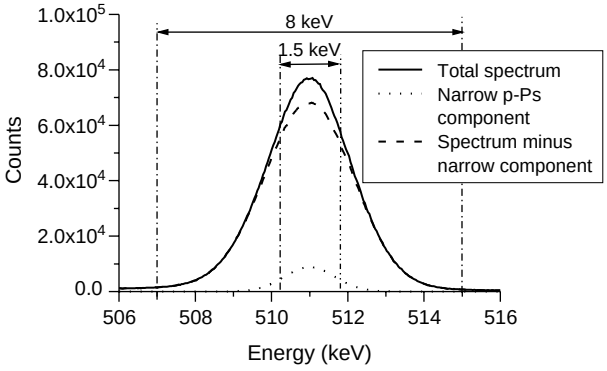

Fig. 2. DBAR spectrum of PMMA showing the contribution to the spectrum from *p*-Ps self annihilation (narrow component) and also the regions of integration used to calculate the *S* and S_b^n parameters. The broad component is calculated as difference between the total curve and the narrow component.

the left and right of the Doppler peak using the routine SPARAM [21]. From this spectra we calculated, as usually, the curve shape parameter *S* as the area of the region around the peak of the annihilation line divided by the total line area. The integration limits were ± 0.75 and ± 4 keV, respectively, around the maximum of the annihilation line at 511 keV. Fig. 2 shows a typical DBAR spectrum after symmetrisation together with these integration limits.

The second step of analysis, we have described in detail in our previous works [9,10]. As we have already mentioned, the DBAR curve can be fitted by a sum of three central Gaussians. The narrowest Gaussian mirrors the self-annihilation of *p*-Ps and the sum of the two wider Gaussians describe the integral effect of e^+ and *o*-Ps pick-off annihilation with electrons of atoms and molecules.

In this work, we used a simplified procedure to separate the narrow component from the wider DBAR curve. First, we calculated the theoretical *p*-Ps DBAR component employing the results from the *o*-Ps annihilation. *p*-Ps, like *o*-Ps, is assumed to be localised in a free volume hole and to occupy the energetic ground state. The width of the narrow component reflects the *p*-Ps confinement momentum and hence the size of the free volume holes. Similarly to Eq. (1), the FWHM of this narrow *p*-Ps component W_n is related to the hole radius by

$$W_n = \frac{6.50}{r_h + \delta r} \tag{2}$$

where, W_n is in kiloelectronvolt, r_h in nanometre and $\delta r = 0.166$ nm [5].

The intensity of the narrow, *p*-Ps, DBAR component, I_n, differs slightly from the *p*-Ps yield ($=1/4P$, *P*—Ps formation probability) due to pick-off annihilation and may be calculated from the equation [1,6]

$$I_n = \frac{1}{4}\frac{P\eta\lambda^o_{p-Ps}}{\eta\lambda^o_{p-Ps} + \lambda_{po}} \tag{3}$$

where, η is the relative contact density (assumed to equal 1 [16]), λ^o_{p-Ps} is the *p*-Ps annihilation rate in vacuum ($=1/125$ ps^{-1}), λ_{po} is the pick-off annihilation rate ($=1/\tau_{o\text{-Ps}}$), and $P = 4I_3/3$.

The energetic resolution function of the DBAR experiments can be well approximated by a Gaussian with a full width of half maximum (FWHM) of 1.30 ± 0.05 keV. The convolution of the narrow DBAR distribution, a Gaussian with a FWHM $= W_n$, results again in a Gaussian, their FWHM can be calculated as the square-root of the sum of both FWHMs squared. Fig. 2 shows the narrow component and the broad component which was calculated as difference between the total spectrum and the narrow component. In our previous works we have shown that this procedure gives very similar but numerically more precise results than an unconstrained three Gaussian fit to the total DBAR curve.

From the broad component we calculated finally the re-normalized curve shape parameter S_b^n as relative area below the broad distribution within the integration limits of ± 0.75 keV (Fig. 2).

3. Results and discussion

Fig. 1 shows the *o*-Ps lifetime τ_3 and the intensity I_3 and Figs. 3 and 4 the DBAR curve-shape parameters *S* and S_b^n as a function of the fractional number f_F of F atoms in our polymers. f_F is calculated as number of F atoms divided by the number of all atoms in the sample. Table 1 compiles the numerical results and shows also the holes radius r_h calculated from τ_3 using Eq. (1).

As can be observed for the copolymer series BMA/HFBMA, MMA/C6FMA, and *t*BMA/C4FMA, the *o*-Ps lifetime τ_3 and the free volume hole radius r_h show a systematic increase with increasing content of fluorinated comonomers. Among the pure methacrylates, PMMA has a lower τ_3 than PBMA and P*t*BMA. The glass transition temperature T_g decreases for MMA/C6FMA from 107 to 83 °C and for *t*BMA/C4FMA from 114 to 101 °C (Table 1). For these polymers the increase in τ_3 correlates well with the decrease in T_g. This corresponds to the behaviour which is

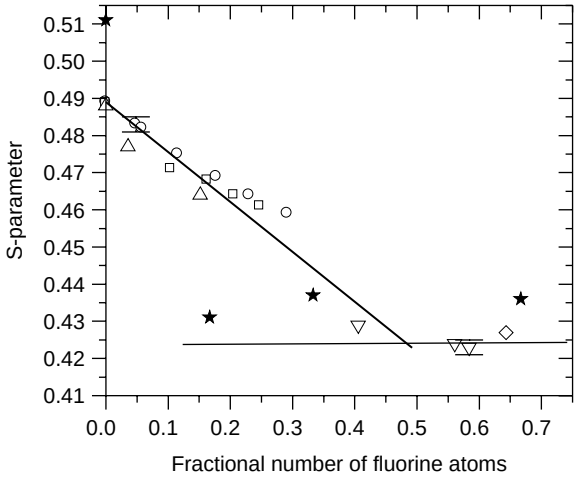

Fig. 3. As in Fig. 1, but the shape parameter of the DBAR curve, *S*. (Empty symbols) amorphous polymers, (filled stars) semicrystalline polymers. The lines through the data are a visual aid.

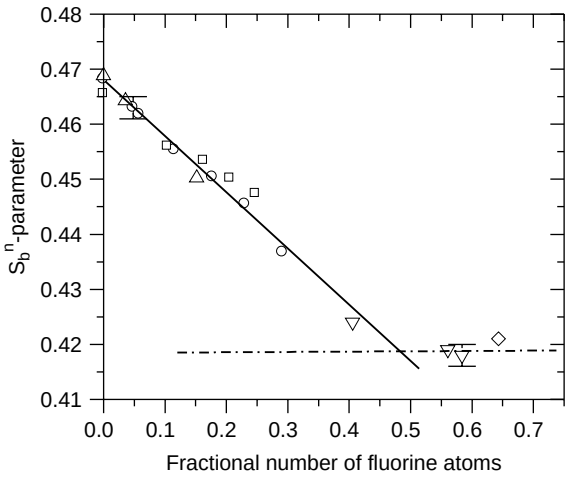

Fig. 4. As in Fig. 3, but the re-normalized curve-shape parameter of the broad DBAR component, S_b^n, for the amorphous polymers. The solid line comes from a linear least-squares fit to the data from below $f_F = 0.45$.

usually observed in the literature for temperatures above T_g [22]. The fluorinated comonomers form sterical hindrances for a dense molecular packing and increase therefore the size of local free volumes. This leads to an increased segmental mobility seen by a decrease of T_g. The reduced molecular packing can be observed also, as in our case, below T_g as an increase in the sizes of local free volume.

For BMA/HFBMA, however, both values, τ_3 and T_g exhibit an increase, T_g from 40 to 56 °C. This may happen when the comonomer reduces molecular packing in the glassy phase, but strengthens the bonding between neighbour chains leading to an increase in T_g.

The vinylidene-based fluoroelastomers VDF/HFP and VDF/TFE/HFP show *o*-Ps lifetimes τ_3 which are smaller than those of the most methacrylate copolymers although their T_g is rather low (between −15 and −18 °C). TFE/PMVE, on the other hand, shows a rather high τ_3 discussed in detail in Ref. [16].

In case of the semicrystalline polymers PE, PVF, PVDF, and PTFE the three-term fit to the lifetime spectrum delivers a lifetime τ_3 which should be considered as an average of *o*-Ps annihilation from the amorphous and from the crystalline phases. At least for PTFE it is well known, that a four-component fit to the lifetime spectrum delivers two *o*-Ps lifetimes, the lower one of ∼1000 ps is attributed to (densely packed) crystals and the higher one of 4100 ps is attributed the amorphous phase [15]. Similar results were obtained for PE [15].

The *o*-Ps formation probability I_3 is highest, ∼30%, for the methacrylates which are free of fluorine. It decreases systematically with increasing fluorine content of the polymers down to values between 10 and 15%. It well known that fluorine may inhibit Ps formation, although the inhibition is not so strong as in case of chlorine, for example [6,23]. This effect may be attributed to the high electronegativity of F atoms and the possible formation of $[F^- – e^+]$ complexes which reduces the number of positrons available for Ps formation. This effect seem to saturate at $f_F > 0.4$ and a typical intensity I_3 of 10–20% is observed for fluorine-rich polymers. In the case of semicrystalline polymers, the integral intensity I_3 may decrease further due to the appearance of crystals which can be observed most clearly for PE and PVF.

Fig. 3 shows that the DBAR curve shape parameter *S* of the amorphous fluorinated polymers (empty symbols) exhibits an approximately linear decrease with increasing fluorine fraction f_F with a levelling-off to a constant lower value for $f_F > 0.5$. The behaviour of *S* shows no correlation with the *o*-Ps lifetime τ_3, respectively, the corresponding free volume hole size but slight fluctuations around the fitted line. The fluctuations have some correlation to the magnitude of the *o*-Ps intensity I_3. This behaviour shows that, almost independently of the structure of the amorphous polymer, the *S*-parameter is controlled by the chemical composition of the material.

The *S*-parameter of PE is distinctly larger than that of the methacrylates. This is mainly due to the presence of oxygen in the methacrylate units which lowers the *S*-parameter compared with a hydrocarbon similarly as fluorine but with a distinctly lower specific effect [9]. Since, the *S*-parameter of the semicrystalline polymers PVF, PVDF, and PTFE is somewhat higher than those of the amorphous fluoropolymers the e^+/Ps annihilation in crystals may also contribute to the high *S*-values of the semicrystalline polymers.

In the following, we discuss the properties of the amorphous fluorinated polymers. The effect of the Ps yield on the curve shape parameter is strongly corrected when calculating the re-normalized curve shape parameter of the broad component, S_b^n. These data show almost the same behaviour as *S* but lower values and less scatter around the fitted curve (Fig. 4). A linear least-squares fit to the data below $f_F = 0.45$ gives

$$S_b^n = 0.468(\pm 0.001) - 0.103(\pm 0.004) f_F. \quad (4)$$

S_b^n is constant at 0.420 above a fluorine fraction of $f_F = 0.5$.

From our previous studies we had expected that S_b^n will show an over-proportionate sensitivity to the presence of fluorine atoms resulting in its steep exponential decrease with increasing fluorine content f_F. The semicrystalline polymers seem to follow this trend. The reason for the linear behaviour of S_b^n for the amorphous copolymers may be found in their chemical structure: the methacrylate units alternate with the semi-fluorinated units which itself have a side chain with a perfluoralkyl tail and a larger part free of fluorine. Due to this structure we may expect that holes occur which have walls free of fluorine atoms and holes, which contain fluorine in their walls. The fraction of the latter type of holes increases with increasing fluorine content of the copolymers leading to the linear decrease of S_b^n with f_F. The copolymers of TFE and VDF with PMVE or HFP and the semicrystalline polymers PVF, PVDF, and PTFE contain not less than one F atom per two backbone carbons. In this case, *o*- the Ps localized at a hole will always find a fluorine atom in whose neighbourhood it will annihilate. This causes the levelling-off in the decrease of the S_b^n.

Our DSC studies showed that the copolymers exhibit a glass transition behaviour which depends strongly on the thermal prehistory of the samples. Well aged BMA/HFBMA copolymers showed during the first heating a single glass transition with strong overshooting due to the enthalpy relaxation. During

the second heating a single glass transition with T_g lower by 2–6 °C was observed. Well aged MMA/C_6FMA- and tBMA/C_4-FMA copolymer samples showed usually indications of two glass transitions which show that the copolymers are in a demixed state. The effects of self-assembly in semifluorinated polymers are discussed in detail in the literature [24,25]. In the second heating, single transitions appeared with widths δT_g between ± 5 and ± 10 °C. We assumed that these samples are in a still mixed or weakly decomposed state and used therefore these samples for the positron studies.

The varying sensitivity of the positron/positronium to the chemical environment around the holes detected previously, which follows the sequence N, O, Cl, and F [9], may be understood in terms of the different electronic configurations of the atoms: H: $1s^1$, C: $2s^22p^2$, N: $2s^22p^3$, O: $2s^22s^4$, F: $2s^22p^5$, Cl: $3s^23p^5$. The higher kinetic energy of the p-electrons leads to a broader momentum distribution (lower S_b^n-parameter) compared to the s-electrons. Although Cl and F contain equal numbers of outer shell p-electrons, the DBAR-spectrum for the fluorine containing polymer is demonstratibly broader than that of the chlorine containing samples [9]. Via 1-dimensional angular correlation of annihilation radiation (1D ACAR) studies, Mogensen [6] demonstrated that the momentum distribution for [e^+, F^-] is significantly broader than that for [e^+, Cl^-]. It is concievable that the origin of the very broad momentum density in the fluorine-polymers and due to this the strong lowering of the S_b^n-parameter is the same as that in [e^+, F^-].

The linear variation of S_b^n with f_F can be also considered as an indication that *o*-Ps stays in that hole where it is formed or trapped first. This conclusion is in agreement with theoretical calculations which show that in amorphous polymers *o*-Ps is bound to a given hole until annihilation due to Anderson-localization [26]. Frequently it is observed that the e^+ lifetime τ_2 shows a similar temperature variation than the *o*-Ps lifetime τ_3 [27,28]. From this observation one may conclude that not only Ps but also positrons (e^+) are Anderson-localized at holes of the free volume until annihilation. For the fluorine elastomers TFE/PMVE and VDF/HFP 22, however, it was observed that τ_2 increases linearly with temperature without response to the glass transition. It was speculated that positrons (e^+, not Ps) may annihilate in the entire empty space (which includes the interstitial free volume) and not only in the holes [16]. Possibly, the high electronegativity of fluorine assists positron localization at smaller empty spaces [29]. The affinity of positrons to F atoms may also enhance the effect of fluorine on the momentum distribution of the copolymers.

4. Conclusions

In this work, we confirmed our previous conclusions that the measurement and evaluation of positron–electron momentum densities via measurements of the DBAR may potentially act as a chemical probe of polymers and other molecular materials. Through, the fitting of three Gaussians, a narrow component arising from *p*-Ps self annihilation, can be identified and subtracted from the total DBAR. A second way, applied in this work, is the calculation of the narrow component from the *o*-Ps annihilation parameters obtained from PALS experiments, τ_3 and I_3, on the same material assuming that the *p*-Ps annihilates in the same free volume holes as the *o*-Ps does. The remaining, after subtraction of the narrow, broader DBAR distribution shows little or no correlation to the spatial dimensions of the free volume holes or the positronium formation probability and shows an enhanced sensitivity to the presence and number densities of various types of atoms in the material.

We focused our activities to fluorinated polymers: three series of copolymers of methacrylates with various semi-fluorinated methacrylates as well as some fluoroelastomers and semicrystalline fluoropolymers. The reason for doing that is that our method shows among various elements its strongest sensitivity for fluorine atoms. We observed that the curve-shape parameter of the broad DBAR component, S_b^n, does not show the expected steep exponential decrease with increasing fractional number of fluorine stoms, f_F, but goes down linearly with f_F in the range $f_F < 0.45$ and levels-off for $f_F \geq 0.5$. S_b^n shows no response to the polymer structure, respectively, the size of free volume holes. As the reason for the linear behaviour of S_b^n may be discussed that, due to the chemical structure of the copolymers, two types of holes may occur: holes which have walls free of fluorine atoms and holes which contain fluorine in their walls. The fraction of the latter type of holes increases with increasing fluorine content of the copolymers. The linear decreases of S_b^n with f_F shows also that Ps does not samples many holes but is localized until annihilation at the hole where it is formed or trapped first. Owing to the local sensitivity, we expect that correlated PALS and DBAR experiments may be a useful tool for studying the self-organization and microphase separation in semifluorinated segmented block copolymers.

The fluoroelastomeric copolymers of TFE and VDF with PMVE or HFP and the semicrystalline polymers PVF, PVDF, and PTFE contain not less than one F atom per two backbone carbons. In this the case *o*-Ps localized at a hole will always find at least one fluorine atom in which neighbourhood it can annihilate. In this case, it can be expected that the parameter S_b^n will show an enhanced, strongly non-linear dependency of the content of fluorine in the polymer as we have concluded in one of our previous works [9].

The information content of this method can be further enhanced through the use of DBAR spectroscopy with two Ge detectors operating in coincidence. This technique is very time consuming, but leads, due to the enormous reduction in the background, to more precise information about the core electron annihilation [12–14] than the conventional single detector DBAR techniques. Such experiments are now in progress.

Acknowledgements

We like greatefully to acknowledge financial support from the EPSRC, UK.

References

[1] Jean YC, Mallon PE, Schrader DM, editors. Principles and application of positron and positronium chemistry. Singapore: World Scientific; 2003.

[2] Xu J, Moxon J. editors. Proceedings of the seventh international conference on positron and positronium chemistry (PPC-7). Rad Phys Chem 2003;68:239.
[3] Faupel F, Kanzow J, Günther-Schade K, Nagel C, Sperr P, Kögel G. In: Positron annihilation, proceedings of the 13th international conference (ICPA-13). Hyodo T, Kobayashi Y, Nagashima Y, Saito H. editors. Mater Sci Forum 2004;445:219.
[4] Pethrik RA. Prog Polym Sci 1997;22:1.
[5] Jean YC. Microchem J. 1990;42:72; In: Positron annihilation, proceedings of the 10th international conference, He YJ, Cao BS, Jean YC. editors. Mater Sci Forum 1995;175–178:59.
[6] Mogensen OE. Positron annihilation in chemistry. New York: Springer; 1995.
[7] Ferry JD. Viscoelastic properties of polymers. New York: Wiley; 1980.
[8] Nagel C, Schmidtke E, Günther-Schade K, Hofmann D, Fritsch D, Strunsky T, et al. Macromolecules 2000;33:2242.
[9] Dlubek G, Fretwell HM, Alam MA. Macromolecules 2000;33:187.
[10] Dlubek G, Alam MA. Polymer 2002;43:4025.
[11] Dlubek G. Mater Sci Forum 1987;13/14:11.
[12] Asoka-Kumar P, Alatalo M, Ghosh VJ, Kruseman AC, Nielsen B, Lynn KG. Phys Rev Lett 1996;77:2097.
[13] Egger W, Bischof G, Gröger V, Krexner G. Mater Sci Forum 2001;363–365:82.
[14] Nagai Y, Nonaka T, Hasegawa M, Kobayashi Y, Wang CL, Zheng W, et al. Phys Rev B 1999;60:11863.
[15] Dlubek G, Saarinen K, Fretwell HM. Nucl Instrum Methods B 1998;142:139.
[16] Dlubek G, Sen Gupta A, Pionteck J, Krause-Rehberg R, Kaspar H, Lochhaas K. Macromolecules 2004;37:6606.
[17] LIFSPECFIT 5.1. Lifetime spectrum fit version 5.1. Laboratory of Physics, Technical University of Helsinki; 1992.
[18] MELT, Shukla A, Peter M, Hoffmann L. Nucl Instrum Methods A 1993;335:310.
[19] Tao SJ. J Chem Phys 1972;56:5499.
[20] Eldrup M, Lightbody D, Sherwood JN. Chem Phys 1981;63:51.
[21] SPARAM. Laboratory of Physics, Technical University of Helsinki; 1989.
[22] Dlubek G, Bamford D, Rodriguez-Gonzalez A, Bornemann S, Stejny J, Schade B, et al. J Polym Sci, Part B: Polym Phys 2002;40:434.
[23] Zhang R, Wu YC, Chen H, Zhang J, Li Y, Sandreczky TC, et al. Rad Phys Chem 2003;68:481.
[24] Hillmyer MA, Schmuhl NW, Lodge TL. Macromol Symp 2004;215:51.
[25] Gottwald A, Pospiech D, Jehnichen D, Häußler L, Friedel P, Pionteck J, et al. Macromol Chem Phys 2002;203:854.
[26] Baugher AH, Kossler WJ, Petzinger KG. Macromolecules 1996;29:7280.
[27] Deng Q, Sundar CS, Yean YC. J Phys Chem 1992;96:492.
[28] Dubek G, De U, Pionteck J, Arutyunov NY, Edelmann M, Krause-Rehberg R. Macromol Chem Phys 2005;206:827.
[29] Dlubek G, Wawryszczuk J, Pionteck J, Goworek T, Kaspar H, Lochhaas K. Macromolecules 2005;38:429.